Thick Filament Substructures in *Caenorhabditis elegans*: Evidence for Two Populations of Paramyosin

Philip R. Deitiker* and Henry F. Epstein*‡

* Verna and Marrs McLean Department of Biochemistry and ‡ Department of Neurology, Baylor College of Medicine, Houston, Texas 77030

Abstract. The thick filaments of the nematode *Caenorhabditis elegans* contain two myosin heavy chain isoforms A and B and paramyosin, the products of the *myo-3*, *unc-54*, and *unc-15* genes, respectively. Dissociation of paramyosin from native thick filaments at pH 6.36 shows a biphasic function with respect to NaCl concentration. Electron microscopy of the remaining structures shows 15-nm core structures that label with monoclonal anti-paramyosin antibody at 72.5-nm intervals. Purified core structures also show 72.5 nm repeats by negative staining. Structural analysis of native thick filaments and dissociated structures suggests that the more dissociable paramyosin is removed radially as well as processively from the filament ends. Minor proteins with masses of 20, 28, and 30 kD cosediment stoichiometrically with paramyosin in purified core structures.

STABLE thick filaments are distinguishing features of the specialized contractile systems of muscle cells. Thick filaments are assemblages of myosin(s), the actin-based motor molecules, which self-associate through the α-helical coiled coils of their rodlike domains. In muscle cells of nonvertebrates, myosin associates with the α-helical coiled-coil protein paramyosin (pm)[1] (Szent-Györgyi et al., 1971) which shares both sequence and structural homology with the myosin rod. In the nematode, *Caenorhabditis elegans*, the combination of genetic, molecular, and structural analysis has been applied to understanding the assembly of thick filaments which contain myosin and pm (Anderson, 1989; Epstein and Fischman, 1991).

Although models for the structure of coiled coils and their self-association by ionic bonds have been presented for myosin and pm (McLachlan and Karn, 1982, 1983; Kagawa et al., 1989), little experimental three-dimensional structural information exists for either individual myosin/pm rods or their organization within the backbones of thick filaments. The lengths (diameters) of thick filaments vary histologically and phylogenetically from 1.53 μm (15 nm) in vertebrates to 10 μm (25 nm) in the nematode *C. elegans* to 30 μm (100 nm) in the barnacle (Levine et al., 1976; Mackenzie and Epstein, 1980). Although these dimensions vary between sources, they are highly homogeneous within each type of muscle cell. Several mechanisms have been proposed to explain the regulation of assembly underlying these phenomena including cumulative strain (Davis, 1986), a vernier between distinct types of copolymerizing molecules (Huxley, 1963), and internal template molecules (Epstein et al., 1985). However, none of these mechanisms have been tested directly with respect to thick filaments. Understanding the substructure of nematode thick filaments seems likely to provide insights into these questions concerning the assembly and interactions of myosin and pm.

The thick filaments of *C. elegans* contain two myosins composed either of *myo-3* encoded myosin heavy chain A (mhc A) or of *unc-54* encoded myosin heavy chain B (mhc B). Mhc A is restricted to the central regions of the filaments (Miller et al., 1983), and *myo-3* null mutants do not assemble thick filaments (Waterston, 1989). Mhc B assembles in the polar regions of the thick filaments (Miller et al., 1983), and *unc-54* null mutants still assemble thick filaments with mhc A substituting along their normal lengths (Epstein et al., 1986). *C. elegans* thick filaments contain pm (Waterston et al., 1974; Harris and Epstein, 1977) which is encoded by *unc-15* (Waterston et al., 1977); *unc-15* null mutants produce abnormal thick filaments with myosins A and B scrambled in the central zones and polar 15-nm wide hollow structures that contain mhc B (Mackenzie and Epstein, 1980; Epstein et al., 1986). Mhc A and pm therefore appear to play critical roles in the assembly of thick filaments in *C. elegans*.

Dissociation of myosin and pm from isolated thick filaments of *C. elegans* produces 15-nm wide hollow structures in which mhc B and pm were not detectable by gel electrophoresis or antibody labeling (Epstein et al., 1985). Importantly, mhc A remains in the central zones. These *C. ele-*

Please address all correspondence to Dr. Henry F. Epstein, Department of Neurology, Baylor College of Medicine, One Baylor Plaza, Houston, TX 77030.

1. *Abbreviations used in this paper*: mhc A, myosin heavy chain A; mhc B, myosin heavy chain B; pm, paramyosin.

gans core structures are similar in appearance to core structures produced from *Limulus* (Levine et al., 1982; 1983; Woodhead, J. L., R. J. C. Levine, and H. A. King. 1986. *J. Cell Biol.* 109:267*a*), however, the *Limulus* structures contain pm. Further analysis of purified native thick filaments from *C. elegans* reveals several additional proteins associated with both intact filaments and core structures (Epstein et al., 1988). However, ~30% of the pm remained with these core structures. These results, therefore, cannot exclude a model in which both pm and additional proteins contribute to the core structure.

In the present work, we have obtained higher yields and purity of thick filaments from *C. elegans* in order to further study the core structure problem. Two populations of pm have been defined on the basis of their differential dissociation. The more soluble pm dissociated with mhc B while the less soluble pm remains associated with mhc A and three minor proteins, P20, P28, and P30 in the core structures.

Materials and Methods

Nematode Growth and Strains

N2 (wild type) *C. elegans* larvae were synchronized by starvation at the L1 stage, and then grown on peptone enriched nematode growth medium for 42 h at 19°C, resulting in a relatively homogeneous L4 population (Schachat et al., 1978; Epstein et al., 1988). Nematodes were washed to remove excess bacteria, purified from debris by density sucrose purification, and washed again five times. Two volumes of O.C.T. (Miles, Ekhart, IN) were added for each gram of nematodes and worms were slowly frozen to −80°C for 30 min and subsequently stored in liquid N_2.

Preparation of Sections

Unless stated otherwise all buffers for isolating and handling filaments contained the following relaxing buffer; 80 mM KCl, 10 mM $MgCl_2$, 1 mM EDTA, 5 mM ATP, 6.6 mM potassium phosphate (pH 6.35 at room temperature). In addition, all buffers contained 1 μg/ml of the following protease inhibitors; chymostatin, pepstatin, leupeptin, soybean trypsin inhibitor (Boehringer-Mannheim Corp., Indianapolis, IN), N-benzoyl-L-arginine ethyl ester (BAEE), and *p*-toluidinyl sulfonyl-L-arginine methyl ester (TAME) (all Sigma Chem. Co., St. Louis, MO). All procedures were performed at 0°C unless otherwise stated. Frozen nematodes were sectioned, and the sections were washed and detergent treated as described previously (Epstein et al., 1988) with the following modifications. Half molar sucrose was added and DTT was not used. Detergent-treated sections were resuspended in 3 ml of a homogenization buffer consisting of relaxing buffer with 0.5 M sucrose, 0.5% Triton X-100 and 1 mM DTT. Sections were homogenized with a glass homogenizer (Wheaton, Millville, NJ) 24 times taking care not to break the surface to produce bubbles or frothing or press the sections against the bottom of apparatus. Sections were pelleted in a 15-ml conical polycarbonate tube (Corning Inc., Corning, NY) in a tabletop centrifuge (IEC, Boston, MA) at setting #3 for 3 min and the supernatant was carefully aspirated and discarded. This limited homogenization was repeated on the pelleted sections twice. The decanted supernatants became less turbid after each homogenization step.

Isolation of Filaments

Prepared sections were resuspended in 4 ml of homogenization buffer and homogenized as described by 600 strokes performed over 1 h. Sections were transferred to a conical 15-ml tube and pelleted in the cold room in tabletop centrifuge at setting #7 for 15 min. The supernatant was carefully removed and placed in a 15-ml polypropylene centrifuge tube (Corning) and cleared in JA-13 rotor (Beckman Instrs., Palo Alto, CA) at 6,200 rpm (6,000 *g*) for 30 min at 4°C. The resultant supernatant (6.2 K supernatant) was carefully removed from top to bottom leaving ~100 μl of supernatant over the pellet. The pellet contained nuclei and chromatin fragments which could trap and aggregate isolated filaments. Isolated filaments were concentrated by spinning the 6.2 K supernatant (3.8 ml) at 11,000 rpm (15,000 *g*) in two thin wall polyallomer centrifuge tubes (Beckman Instrs.) in a SW 50.1 rotor at 2.5°C (15 K pellet). Table I shows the several steps in the purification of thick filaments as monitored by myosin, pm, and associated proteins.

Dissociation of Filament Proteins by Titration with NaCl and pH

Pelleted isolated filaments (15 K pellet) from 2 gm of nematodes were resuspended in 500 μl of relaxing buffer (containing 0.5 M sucrose and 1 mM DTT), and divided equally between 14 microcentrifuge tubes. Filaments were repelleted 30 min at 12,000 rpm in a JA-13 rotor, and the supernatant discarded. 1 ml of dissociation buffer was formulated as follows. 200 μl of 5× relaxing buffer stock was mixed with 5 M NaCl and double distilled H_2O to achieve the desired final salt concentration. For samples in which the pH was elevated, 33 mM phosphate in the 5× relaxing buffer stock was substituted with 20 mM glycine, 20 mM MES, 20 mM MOPS, and 20 mM Tricine resulting in a solution with a broad range of buffering capacity. The pH was adjusted with NaOH at room temperature. 80 μl of dissociant (0°C) was added to samples, repipetted vigorously, and allowed to sit 5 min on ice. Samples were spun in the same tube for 70 min at 12,000 rpm in a JA 13 rotor.

Purification of Filaments on Analytical Sucrose Gradients

Each 15 K pellet was vigorously resuspended in 1 ml of filament compatible buffer suitable for DNase I digestion (72 mM NaCl, 3 mM $MgCl_2$, 3 mM ATP, 0.5 M sucrose, 15 mM Tris-HCl, pH 6.5). Approximately 1 mg of bovine pancreatic DNase I (protein grade, Pharmacia LKB Biotechnology, Piscataway, NJ) was sprinkled onto 1 ml of buffer and allowed to dissolve. The solution was carefully repipetted with a wide bore pipette and 500 μl was carefully added to each tube of resuspended 15 K pellet and allowed to incubate 20 min at room temperature. Each tube was chilled on ice and carefully layered onto an 18 ml, 18–33% (wt/vol) velocity sucrose gradient made with relaxing buffer containing 1 mM DTT. Gradients were spun for 9 h at 7,000 rpm in an SW 28 rotor at 2.5°C. Filament purification is markedly improved by longer spins at $g < 10{,}000$. Gradients were fractionated from the bottom into 12 fractions. Equivalent fractions were pooled from the gradients, and filaments were pelleted in polyallomer tubes in SW 50.1 at 20,000 rpm for 5 h. Pellets were solubilized in sample dilution buffer and separated on 6–12% polyacrylamide gels.

Purification of Filaments on Preparative Sucrose Gradients

5 ml of isolated filaments (6.2 K supernatant) were loaded per 9 ml 18–33% sucrose gradient and spun in 38 ml polyallomer centrifuge tube (PGC, Gaithersburg, MD) with a SW 28 rotor at 4,000 rpm for 12 h at 2.5°C. A single 5 ml fraction starting at 2.5 ml from the bottom of the gradient was removed.

Repurification of filaments on Sucrose Gradients

For repurification of dissociated filaments, KCl was replaced by the more powerful dissociant KSCN. 50 mM KSCN achieves the same level of dissociation as 400 mM NaCl. 7.6 ml of filaments purified on preparative gradients were dissociated by slowly adding 3.8 ml of a solution containing 120 mM KSCN and 150 mM Tris-HCl, pH 7.5. Dissociation filaments were layered onto six 18–33% sucrose gradients containing 100 mM NaCl, 1 mM $MgCl_2$ 3 mM ATP, 1 mM DTT, and 25 mM Tris-HCl (pH 7.5). Gradients were spun, fractionated, and analyzed as described for analytical purification of filaments with the exception of the 32 h run time. Fractions were pelleted at 25,000 rpm for 9 h. As a control, native filaments were repurified by diluting 7.6 ml of filaments purified on preparative gradients with 3.8 ml of relaxing buffer containing 1 mM DTT. Diluted filaments were loaded onto three 18 ml gradients, spun, fractionated, and analyzed as described for analytical purification of filaments.

Analysis of Myosin Solubilized during Filament Isolation

Soluble myosin in the 6.2 K supernatant was separated from filament bound myosin by layering 700 μl of supernatant (differs from supernatants described above with respect to added 1 mM PMSF) on a 2.5-ml 18–33% native gradient also containing 1 mM PMSF. Filaments were pelleted through the gradient by centrifugation in SW50.1 rotor at 8,000 rpm for 15 h. 1.5 ml was removed from the top of the gradient and immediately treated with 0.38 ml of SDS sample buffer. The gradient pellet was resuspended in 1.875 ml of sample buffer. Equal volumes of supernatant and pellet were loaded onto SDS-PAGE and the resulting amounts of myosin determined by densitometry.

Gel Electrophoresis

The gel electrophoresis, Coomassie-blue staining, and destaining protocols used were as previously described (Epstein et al., 1985, 1988) with the following modifications. Samples were loaded with a buffer containing 3% glycerol. With the exception of untreated sections, which were immediately solubilized by heating 90 s in boiling water, all samples were heated at 80°C for 10 min before loading. Electrophoretic current was kept at 7 mA (40 V) until dye front had moved half the distance of the gel, after which current was increased to 20 mA. Gels were stained and destained in a solution of 45% methanol, 10% acetic acid. Densitometry of Coomassie-blue stained bands was analyzed using a model 620 Videodensitometer (Bio-Rad Labs., Richmond, CA). Linearity over a 20-fold range of Coomassie-blue stained protein was achieved by determining the "cross-product area" of each band. The maximal horizontal distance and the central vertical distance was determined for each band, and their product calculated.

Electron and Immunoelectron Microscopy

Procedures for electron microscopic examination of native- and antibody-labeled thick filaments has previously been described (Epstein et al., 1985; Miller et al., 1983). Monoclonal antibodies 5.6 (anti-mhc A), 28–2 (anti-mhc B), and 5–23 (anti-pm) were reacted at 1, 10, and 50 μg/ml, respectively. The secondary antibody, affinity-purified goat anti-mouse (Cappel Luss, Durham, NC) was used at 20 μg/ml. Electron microscopy of purified materials were prepared from unpelleted gradient fractions. Length determinations of native and dissociated filaments were made by measuring lengths on photographic enlargements of electronmicrographs. Magnifications were calibrated with catalase crystals. Structures (native or dissociated) were classified into three groups based upon the degree of anti-mhc A labeling: no label, label at one end but not exhibiting a complete central zone, and structures with full length central zones (1.8 μm).

Results

Improved Isolation of Thick Filaments

Fig. 1 shows the protein compositions of the early steps in isolating thick filaments from *C. elegans*. The initial homogenization preferentially removed nuclei and ribosomes from the sections (compare Fig. 1 *B* to Fig. 1 *C*). The sections were then more extensively homogenized with smaller amounts of nuclei and ribosomes still being released as evidenced by histones and ribosomal proteins. The extract was clarified of large aggregates of various structures including filaments, nuclei, and debris by sedimentation at 6,200 *g* (6.2 K supernatant). The protein composition of the 6.2 K supernatant was very similar to the composition of the 3× homogenized sections shown in Fig. 1 *C*. Thick filaments can be concentrated by centrifuging the 6.2 K supernatant at 15,000 *g* and collecting the thick filament-containing 15 K pellet (Fig. 1 *D*). Thin filaments, ribosomes, and other species of lower S value were enriched in the 15 K supernatant. Thick filaments and core structures were further purified on gradients for certain experiments (see below).

Dissociation of Paramyosin from Thick Filaments

The dissociation of the three major body wall thick filament proteins mhc A, and mhc B, and pm with KCl has been examined previously leading to the identification of core structure (Epstein et al., 1985). From those experiments, it appeared that myosin and pm were extracted almost completely from filaments at 400 mM KCl. A smooth core structure with a thickened central region that reacts with anti-mhc A antibodies remained. However, the smaller amounts of filaments then available and increased levels of impurities interfered with the analysis of low levels of pm by gel electrophoresis and densitometry. Current dissociation experiments (Fig. 2) treating more highly purified filaments with a mix-

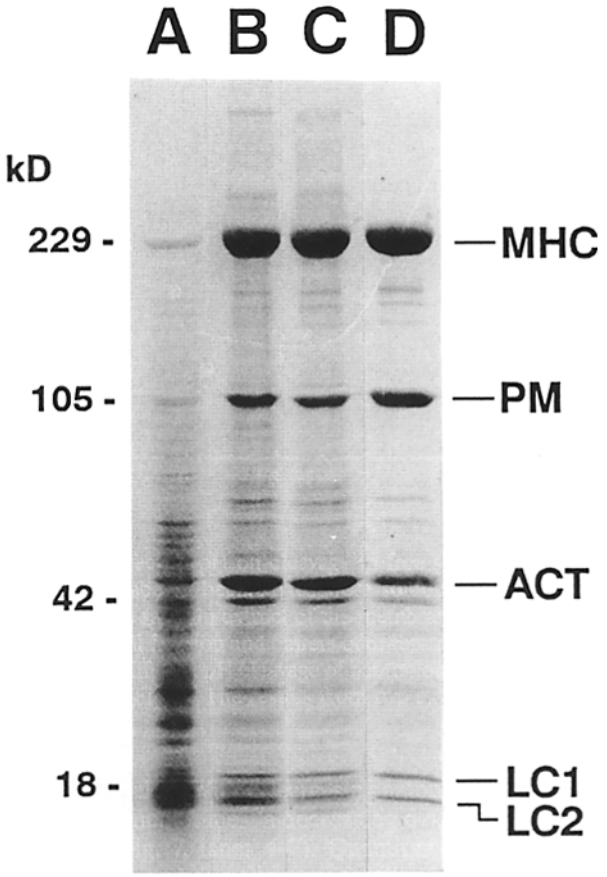

Figure 1. Gel electrophoresis of selected steps in the enrichment of thick filaments. (25 μg of total protein per lane). Limited gentle homogenization before isolation resulted in sections enriched in filaments. Untreated section (*A*), Triton X-100-treated sections (*B*), 3× homogenized pellet (*C*), and isolated filaments pelleted to reduce actin and ribosomal contaminants (*D*).

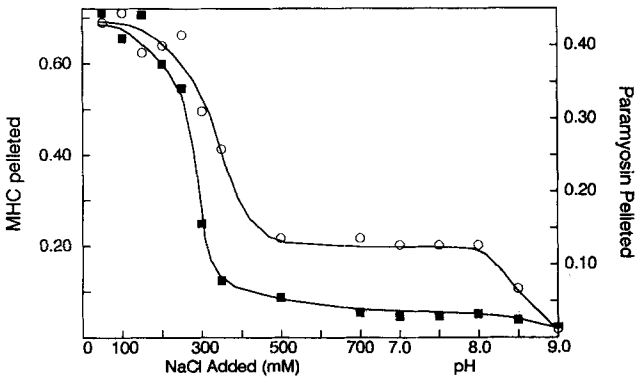

Figure 2. Dissociation of myosin heavy chains and paramyosin from thick filaments. 15 K pellet filaments were aliquoted and repelleted. Pellets were resuspended with modified buffer, which had additional NaCl as described along X-axis. In addition, some samples were subjected to NaCl treatment (700 mM) at elevated pH. All samples were repelleted 1.1 h at 12,000 rpm. Myosin heavy chains (*closed squares*) and pm (*open circles*) were quantitated by video densitometry of Coomassie blue-stained SDS gels.

ture of 100 mM KCl and added NaCl resemble the previous work in that a majority of both myosin and pm are extracted from filaments with 500 mM mixed salt concentration (NaCl is a slightly milder dissociant than KCl). However, at concentrations of mixed salt greater than 500 mM (pH 6.35) and less than 800 mM (pH 8.0), a plateau level of pm (~30%) remains pelletable. The sedimentation of soluble pm, with a sedimentation coefficient of less than 4, cannot account for this plateau. Comparison of these results with previous experiments indicated that the pm-containing structures remaining at plateau conditions were likely to be core structures.

Core Structures Contain Paramyosin

Native filaments were incubated with 400 mM NaCl–100 mM KCl, pH 6.34, leading to partial dissociation and examined by electron microscopy. Fig. 3 *A* shows an untreated native filament obtained from the 15 K pellet with a diameter of 25 nm. Dissociated structures (Fig. 3 *B*) showed the same diameter as previously described for core structure (15 nm) (Levine et al., 1982). A faint repeat of 72.5 nm was visible in the dissociated structures.

The core structures were reacted with anti-pm monoclonal antibody (mAb 5–23) at 50 μg/ml followed by secondary antibody in order to verify the existence of pm on dissociated structures. Lower concentrations of anti-pm, 1.0 and 10.0 μg/ml, do not detectably label the core structures (Epstein et al., 1985). Fig. 3 *C* shows the strong reaction of these antibodies at regular 72.5 nm intervals along the dissociated structures. This monoclonal antibody did not label native filaments under conditions that the anti-mhc A and anti-mhc B labeled (data not shown). Neither secondary antibody alone reacted with core structures and secondary anti-mhc B (mAb 28.2). Anti-mhc A (mAb 5.6) labeled the central regions of core structures verifying previous work (Epstein et al., 1985). The locations of the anti-pm reactions indicated that core pm may extend to the central mhc A-containing regions of core structures (Epstein et al., 1985).

Length and Symmetry of Filaments and Core Structures

Previous results of this laboratory show that the average length of isolated core structures, 3.2 μm, was significantly shorter than the initial native thick filaments, 7.3 μm (Epstein et al., 1985, 1988). Our previous models for filament dissociation proposed that pm dissociates radially. However, the present observation that the less dissociable pm is the major component of a shortened substructure raises the possibility that the more dissociable fraction of pm could have been removed processively from the ends of filaments. A second mechanism for the shortening of core structures is mechanical shearing.

To distinguish between these mechanisms for pm dissociation and reduction in the lengths of structures, both isolated native thick filaments and dissociated core structures were analyzed in terms of their overall lengths, the presence of intact central mhc A-containing zones, and the symmetry of the overall structure about these zones. The central zones were identified by reaction with anti-mhc A (mAb 5.6) which produces prominent labeling of the central 1.8 μm zones of native filaments (Miller et al., 1983). The very center of these mhc A-containing zones, the 0.15 μm long structural bare zone which contains only the rods of myosin molecules, remains unlabeled because mAb 5.6 reacts with the S2 hinge region of mhc A (Epstein et al., 1986). Structures that did not contain these zones or only incomplete ones were con-

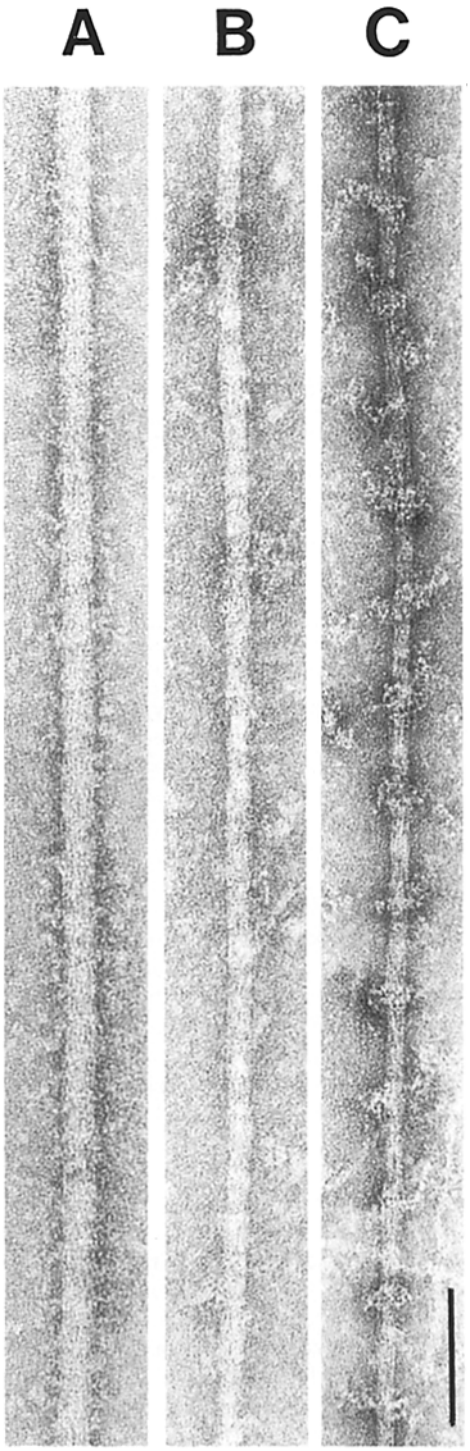

Figure 3. Labeling of core structures by anti-pm. 15 K pelleted thick filaments (*A*) were treated with 500 mM mixed NaCl-KCl, pH 6.35 (*B*), and then reacted with 50 μg/ml monoclonal antibody (mAb 5.23) followed by 20 μg/ml affinity-purified goat anti-mouse secondary antibody (*C*). Samples were negatively stained with 2% uranyl acetate and viewed by electron microscopy. Bar, 100 nm.

sidered to be products of shearing. The remaining structures were considered to be products of dissociation; symmetrical filaments and core structures could be the products of processive and/or radial dissociation. These possibilities were distinguished by comparing the lengths of the initial filaments and dissociated core structures. The distribution of pm along the long axis was assumed to be uniform for the calculations below.

Fig. 4 *A* shows the lengths and central zone characteristics of isolated thick filaments. The mean length of filaments with complete central zones was 7.1 μm. This length, itself, is shorter than the 9.7 μm length estimated from polarized light microscopy from body-wall muscle A bands in situ (Mackenzie and Epstein, 1980) and may result, in part, from the processive solubilization of 22% of myosin, predominantly mhc B (see below), during isolation. Shearing also plays a role since 6.5% of the filaments lack centers, and the filaments with centers exhibited some lack of symmetry (Fig. 4 *C*).

The average length of dissociated structures was 3.2 μm (Fig. 4 *B*). However, 27% did not show mhc A-labeled central zones. The dissociated structures with complete central zones showed a mean length of 3.9 μm and a small deviation from symmetry similar to that of the isolated filaments (Fig. 4 *D*). These experiments indicated that the lengths of core structures with centers were 55% of the lengths of the original isolated filaments with centers and represented 89% of the mass of total core structures based upon the length distribution. Processive loss of length alone or together with shearing (11% of the mass) cannot, therefore, numerically account for the dissociation of 70% of pm from the initial filaments. We conclude that a significant fraction of pm dissociated radially in the production of core structures in addition to processive dissociation and shearing.

Purification of Native Filaments

The dissociation experiments as monitored by gel electrophoresis and electron microscopy suggested the presence of two populations of pm in thick filaments. Pm molecules in the more readily dissociated population may associate with myosin molecules of the filament cortex and other pm molecules whereas pm molecules in the less dissociable population would be associated within the core structures. One possible explanation for decreased dissociation of the internal population may be the presence of additional proteins which interact with the pm in the core structures. Sedimentation on velocity sucrose gradients has been used previously in order to search for minor thick filament proteins (Morimoto and Harrington, 1973; Epstein et al., 1988); however, because of the smaller amounts of isolated filaments available in the 1988 nematode experiments, it was not possible to isolate and purify a sufficient quantity of structures for the clear identification of proteins by Coomassie blue staining.

The improved isolation procedure described above is suitable for the higher yield purification of filaments (Fig. 5 *A*). The results of this purification are similar to those described previously, but resulted in about 23 μg of highly purified thick filaments from each gram of nematodes (Table I). Fig. 5 *A* (lanes *5–8*) show that the peak fractions containing thick filament-associated myosin and pm were well separated from structures of lower S value and allowed the detection by Coomassie blue staining of thick filament-associated minor proteins present at levels of 1% or greater.

A number of minor proteins consistently copurified with thick filaments (Fig. 5 *A*). By SDS-PAGE, a set of protein bands were detected between myosin and pm. Their levels

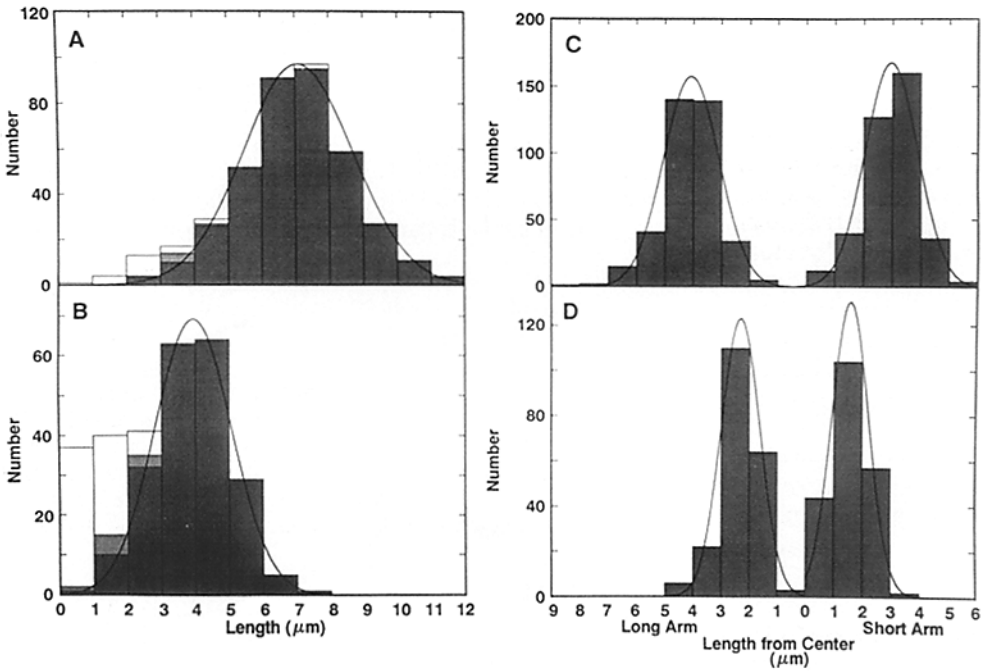

Figure 4. Length and symmetry of filaments and core structures. 15 K pelleted thick filaments and 15 K pelleted thick filaments dissociated by adding 400 mM NaCl were allowed to attach to grids and subsequently reacted with mAb 5.6 (anti-mhc A) followed by secondary antibody. Histograms of lengths of native filaments (*A*, n = 403) and dissociated structures (*B*, n = 280) are subdivided into three groups: structures that lack antibody labeling (*white*), structures with some antibody labeling but lack true central zones (*grey*), and structures with complete central zones (*dark grey*). The symmetry of the structures which contain centers was analyzed by plotting length of the longest arm left of the origin and the length of the shortest arm right of the origin for both native (*C*) and dissociated (*D*) filaments. Note that the Gaussian curves and means were calculated from the total data whereas the histograms were constructed by grouping the data into the indicated bins.

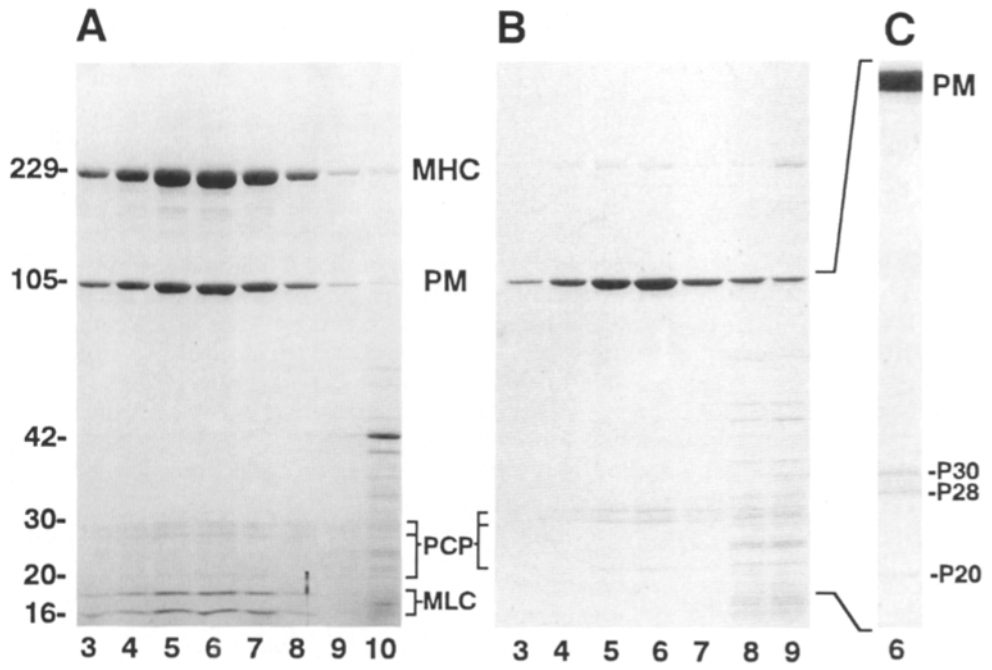

Figure 5. Purification of native filaments and core structures: demonstration of minor core associated proteins. Both native filaments (*A*) and core structures (*B*) were purified on four parallel 18 ml 18–33% sucrose gradients at 7,000 rpm. Native filaments (15 K pellet) sedimented for 9 h at a distance consistent with 500 S particles. Core structures (KSCN dissociated filaments from preparative gradients) sedimented for 32 h at a distance consistent with 150 S particles. Single lane (*C*) is an enlargement of lane *B6* showing three putative core structure-associated proteins. Putative core proteins (*PCP*) refer to the subset of minor components which are found in both native filaments and core structures.

correlated with the amounts of myosin heavy chain present. In immunoblots, these bands label with either anti-mhc A or anti-mhc B (data not shown). Previous experiments demonstrated that the nematode homogenates when analyzed immediately lack these bands, suggesting that these proteins are breakdown products of myosin heavy chains. The gel region between pm and the myosin light chains (Fig. 5 *A*) contained a prominent band at 28 kD, two prominent bands at 30 kD, and two faint bands at ~20 and 32 kD. Monoclonal anti-myosin and anti-pm antibodies did not show reaction with any bands in this region (data not shown).

Purification of Dissociated Filaments

Because the majority of myosin and pm molecules have been dissociated, core structures should have a significantly lower S value than native filaments. Therefore, sedimentation velocity experiments would be useful for separating core structures and their associated proteins from other species. Although NaCl was useful in titrating the dissociation of thick filaments, filaments dissociated in NaCl aggregate upon sedimentation into higher S value complexes. KSCN, a stronger dissociant, does not result in the large scale aggregation of unpelleted structures. Densitometric analysis of pelleted core structures generated by 50 mM KSCN and 500 mM mixed chloride salts (100 mM KCl, 400 mM NaCl) demonstrated that conditions were comparable, and 50 mM KSCN was used to dissociate native filaments in order to produce purifiable cores.

To preselect only thick filament-associated proteins, thick filaments were first partially purified on preparative gradients. In such preparations, five minor protein bands between 20–32 kD were prominent. Thick filaments were then dissociated with 50 mM KSCN and resedimented over a second set of gradients. Fig. 5 *B* shows that at the same rotor speed, dissociated filaments required 32 h to sediment a distance traveled in 9 h by native filaments. As a control, native filaments were repurified on similar gradients and showed an identical mobility to 15 K pellet filaments. This experiment suggested that the apparent sedimentation constant of 500 S

Table I. Isolation and Purification of Thick Filaments

	Total protein (*mg*)	Myosin* (*mg*)	PM (*mg*)	TFAP‡ (*mg*)	TFAP‡ (%)	Fold purification
Untreated sections§	108	3.10	1.15	4.77	4.4	1.0
Triton X-100 pellet	20	3.10	1.15	4.77	23.8	5.4
3X Homogenized pellet	13	2.34	0.80	3.52	27.1	6.2
15 K × g Pellet of isolated filaments	0.80	0.23	0.11	0.382	47.8	10.9
Gradient purified filaments	0.026	0.012	0.0067	0.023	92.4	21.0

* Myosin values represent the sum of myosin heavy chains and light chains.
‡ TFAP, thick filament associated proteins (Myosin, pm and PCPs), the values obtained for putative core proteins (PCP) in the purified filaments are used in evaluating TFAP and are assumed to be a fixed ratio relative to myosin and pm.
§ Because the level of nonfilament associated proteins in the whole homogenate obscures the densitometric measurement of myosin and pm, the total amount of individual TFAPs are assumed to be the same as the TX-100 pellet.

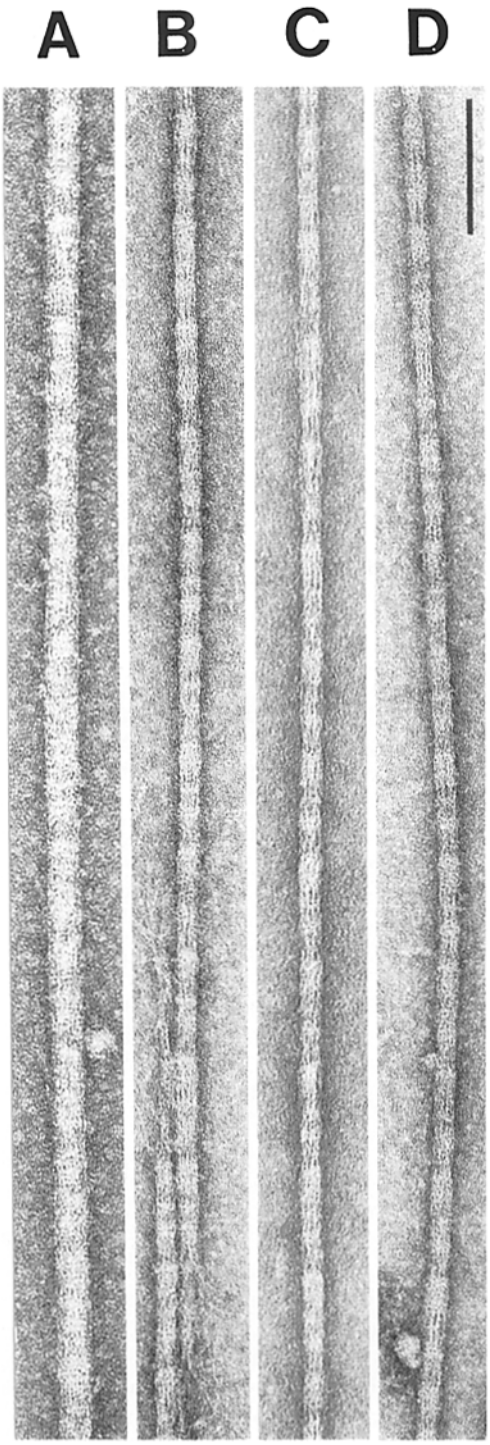

Figure 6. Electron microscopy of purified filaments and core structures. Gradient purified core structures (*B–D*) are compared with purified native filaments (*A*). Samples were negatively stained with 2% uranyl acetate. Bar, 100 nm.

for native filaments was reduced substantially upon partial dissociation to an apparent 150 S for the core structures. The existence of core structures within the peak fractions was confirmed by electron microscopy (Fig. 6, *B–D*).

The myosin and pm in the cortex of purified thick filaments appear to have 1:1 stoichiometry, however, this result must be interpreted cautiously. Densitometric analysis of nonfilament containing supernatants of native filament extracts demonstrate that 22% of myosin is solubilized during isolation and purification. Summing the soluble myosin and the fraction of assembled myosin in the isolated thick filaments results in a molar ratio of myosin to paramyosin of 1.0:1.2. This value is similar to the ratio of A and B myosin heavy chains:pm (mol/mol) of 1.0:1.1 measured previously by densitometry of immunoblots of L4 worm homogenates (Honda and Epstein, 1990).

Several Polypeptides Are Associated with Purified Core Structures

SDS-PAGE of the fraction most enriched in core sedimentation velocity gradient was analyzed by densitometry in order to determine the relative proportion of protein constituents. Myosin, as monitored by myosin heavy chain, was present at 5% and pm at 69% by weight of total Coomassie blue-stained material. Fig. 5 *C* shows that only three of the five previously noted thick filament-associated polypeptides were enriched with the core structures. The three polypeptides at 30, 28, and 20 kD account for 10, 11, and 5% of core protein mass, respectively, and would exist in core structures at molar ratios to molecular pm (a dimer of two 100-kD polypeptides) of 1.0, 1.2, and 0.80, respectively (Table II).

Electron Microscopy of Purified Core Structures

In contrast to previous work with more heterogeneous material, purified core structures showed a pronounced repeat of 72.5 nm containing three subregions of low stain penetration (Fig. 6, *B–D*). These repeats were relatively faint in purified native filaments (Fig. 6 *A*). Along the length of many core structures, regions in which four or more longitudinal, stain-excluding strands could be observed in projection, but their location did not precisely coincide with the 72.5 nm repeats. By inspection, the pattern of the repeats was clearly polar.

Discussion

We have reexamined the complex substructure of thick filaments and their core structures in *C. elegans*. With the avail-

Table II. Polypeptide Components of Thick Filaments and Core Structures

Polypeptide	Thick filament	Core structure	Soluble
Mhc A and B*	2.88	0.035	2.85
Pm	3.3	1.0	2.3
P32	0.29	–	0.29
P30a	0.5	0.5	–
P30b	0.5	–	0.5
P28	0.65	0.65	–
P20	0.42	0.42	–
MLC	2.88	0.035	2.85

Values represent the molar ratio of filament polypeptides to core pm polypeptide. Values for MLC are based upon myosin heavy chains. Actual stoichiometric relationship of associated core proteins may be doubled since both myosin heavy chain and pm exist as dimers.
* Myosin value is the summation of filament bound myosin as well as myosin released upon isolation.

ability of increased amounts and purity of nematode thick filaments, titration with salts and pH distinguishes two populations of pm based upon their differential dissociations. The less dissociable population of pm, ~30% of the total, is the major protein component of core structures. Processive loss of pm from filament ends cannot fully explain the 70% dissociation of pm since the resulting core structures show 55% of the lengths of isolated thick filaments. A significant portion of the pm, ~45%, must be dissociated by other mechanisms. Radial dissociation of this pm appears to be the most likely alternative mechanism while the contribution of shearing is relatively minor. The presence of pm has been verified by labeling with anti-pm antibodies at regular intervals of 72.5 nm in all but the most central regions of isolated core structures. Native thick filaments react along their entire lengths with anti-pm mAb except for their central zones in immunofluorescence microscopy experiments (Epstein et al., 1993). This finding is consistent with our assumption of a uniform distribution of pm in the polar regions of thick filaments in order to estimate radial and longitudinal dissociation of pm. Our calculations of radial dissociation may be *underestimates* rather than *overestimates* because the clear tapering of the thick filaments suggests that there may be less non-core paramyosin near the poles than towards the center of the filaments (Epstein et al., 1985).

The greater yields and purification of thick filaments than obtained previously (Epstein et al., 1985, 1988) allow the identification of three proteins with M_r's of 20, 28, and 30 kD as additional putative components of core structures. These polypeptides are detectable by Coomassie blue in the current samples of purified core structures whereas in the previous preparations of thick filaments, the lower levels of additional bands required silver staining for their detection. P20, 28, and 30 differ from all but possibly polypeptide j previously described (Epstein et al., 1988). The other polypeptides in the 100–200-kD range are cross-reactive with anti-mhc A mAb as detected by sensitive alkaline phosphatase-linked secondary antibody (Deitiker, P. R., D. L. Casey, and H. F. Epstein, unpublished work). A polyclonal antiserum has been raised to P28; this antibody reacts with P28 but not pm on immunoblots (Deitiker, P. R., and H. F. Epstein, unpublished results). The very large gene product of *unc-22* in *C. elegans*, twitchin, is detectable in purified thick filaments only at low levels by immunoblots with anti-twitchin antibody; most of the twitchin cosediments at about 11S with the nonfilamentous 22% of myosin (Valenzuela, M., P. R. Deitiker, H. F. Epstein, and G. Benian, unpublished results). The apparent stoichiometries of the 20, 28, and 30 kD polypeptides with core pm molecules are about 1:1:1:1. The purification of core structures has allowed the visualization of 72.5 nm axial repeats reminiscent of the well known paracrystalline organization of pm as well as more complex substructures that require further elucidation.

The presence of pm in core structures modifies the model of filament structure (Fig. 7) that proposed the coaxial assembly outside to inside of myosin, pm, and a non-pm core structure (Epstein et al., 1985). However, the existence of two populations of pm may be related to two sets of differential interactions of pm with other proteins as well as with itself (Epstein et al., 1988). The more easily dissociable pm would interact primarily with myosin molecules in the thick filament cortex and secondarily with the underlying core structures. The less easily dissociable pm would interact primarily with other pm molecules and possibly, the associated core proteins P20, P28, and P30. The information regarding pm in this report is limited to the mhc B-containing polar regions of nematode thick filaments. The composition and organization of the filament backbones in the mhc A-containing central zones is not known.

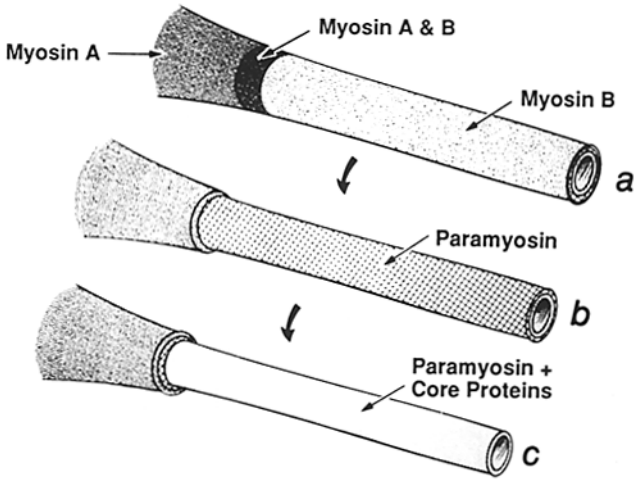

Figure 7. Model of thick filament substructures in *C. elegans*. One half of a filament is depicted schematically. (*A*) The myosin cortex with its central mhc A zone and its polar mhc B zone. (*B*) The more dissociable paramyosin compartment. (*C*) The core structure containing the less dissociable paramyosin and the putative core proteins.

The two populations of pm might also differ at the level of posttranslational modification. Previous work suggests that nematode pm exists in several phosphorylation states (Schriefer and Waterston, 1989) and that the cortical pm is phosphorylated preferentially upon solubilization whereas the remaining core structure pm does not readily accept phosphoryl transfer in vitro (Dey et al., 1992). The differences between the two pm populations in both their assembly and dissociability may possibly be related to differential phosphorylation.

Genetic results also suggest the possible role of modification in the assembly of thick filaments. The pm in *unc-82* mutants has been reported to show altered phosphorylation (Schriefer and Waterston, 1989). *Unc-82* mutants also produce multifilament assemblages similar to those of *unc-15* mutants with changes in single charges (Epstein et al., 1987). These observations suggest that the model of Gengyo-Ando and Kagawa (1991) in which the *unc-15* mutations reduce the stability of myosin-pm interactions normally within wild-type thick filaments and thereby enhance the pm–pm interactions that are predominant in the mutant multifilament assemblages could also apply to the *unc-82* mutations. These considerations would provide additional support for a possible role of phosphorylation in the formation of myosin-pm interactions within the more cortical regions of the thick filament.

The possibility that alternative pm isoforms exist as in *Drosophila* (Becker et al., 1992) cannot be formally excluded. However, there appears to be only one major mRNA species encoding pm by Northern blot analysis (Honda and Epstein, 1990; Kagawa et al., 1989). Since the *e1214* premature chain termination allele of *unc-15*, the known nematode pm gene, shows complete or nearly complete loss of pm

(Waterston et al., 1977; Mackenzie and Epstein, 1980), there does not appear to be a second gene that could encode 30% of the pm.

The polar arrangements of 72.5 nm repeats in the electron micrographs of the anti-pm antibody-labeled isolated core structures and the negatively stained purified core structures are consistent with the P1 arrangement proposed for synthetic paracrystals of purified pm (Cohen et al., 1971, 1987), with the prediction of optimal stagger between pm molecules based upon analysis of the amino acid sequence (Kagawa et al., 1989), and the distance in the sequence between the single charge mutation *e73* and its revertant *m209* (Gengyo-Ando and Kagawa, 1991). However, each 72.5 nm repeat in the nematode core structures contains three sub-regions of differing lengths that exclude negative stain. This pattern appears more complex than the simple alternation of stained and stain-excluded subregions seen with the P1 paracrystals. In one of these subregions, a number of strandlike structures (most usually four) are seen. These strands may represent projections of subfilaments composed of coiled-coil pm rods. The relative complexity of these patterns compared to those of synthetic paracrystals of purified pm may be caused by interactions of the pm with the additional proteins of the core structures. Preliminary three-dimensional reconstructions of these electron micrographs of purified core structures suggest the presence of globular proteins inside sheaths of helically arranged paramyosin-containing subfilaments (Schmid, M., G. Lu, P. R. Deitiker, I. Ortiz, and H. F. Epstein, unpublished results).

The present results provide a basis for further understanding of the roles of the core proteins pm, P20, P28, and P30 in the assembly and three-dimensional structure of thick filaments. The molar stoichiometry of dimeric pm molecules to the associated core polypeptides is consistent with the latter acting as molecular cross-linkers of pm within the core structure. Our model is distinct from the proposals for the subfilaments of scallop striated muscle thick filaments which may contain myosin, pm, and high molecular weight accessory proteins (Vibert and Castellani, 1989; Castellani and Vibert, 1992). The production of specific antibodies to P20, P28, and P30 may permit verification of their location in the core structures and characterization of their sequences through molecular cloning. Further analysis of the phosphorylation of pm is needed to clarify the role of this modification in thick filament structure and assembly. The availability of purified core structures with evident periodic substructures may permit more detailed structural analysis of the molecular interactions within the backbones of thick filaments of *C. elegans*.

This paper is dedicated to the memory of Professor William F. Harrington who encouraged us in this work. We are indebted to our colleagues Irving Ortiz, Douglas Casey, Michael Schmid, and Wah Chiu for assistance, encouragement, and suggestions. Ritesh Mathur contributed to the filament purification experiments.

This research was supported by grants from the National Institute of General Medical Sciences and the Muscular Dystrophy Association.

Received for publication 11 December 1992 and in revised form 6 July 1993.

References

Anderson, P. 1989. Molecular genetics of nematode muscle. *Annu. Rev. Genet.* 23:507–525.

Becker, K. D., P. T. O'Donnell, J. M. Heitz, M. Vito, and S. I. Bernstein. 1992. Analysis of *Drosophila* paramyosin: identification of a novel isoform which is restricted to a subset of adult muscles. *J. Cell Biol.* 116:669–681.

Castellani, L., and P. Vibert. 1992. Location of paramyosin in relation to the scallop striated muscle. *J. Muscle Res. Cell Motil.* 13:174–182.

Cohen, C., A. G. Szent-Györgyi, and J. Kendrick-Jones. 1971. Paramyosin and the filaments of the molluscan "catch" muscles. I. Paramyosin: structure and assembly. *J. Mol. Biol.* 56:223–237.

Cohen, C., D. E. Lanar, and D. A. D. Parry. 1987. Amino acid sequence and structural repeats in schistosome paramyosin match those of myosin. *Biosci. Rep.* 7:11–16.

Davis, J. S. 1986. A model for length-regulation in thick filaments of vertebrate skeletal myosin. *Biophys. J.* 50:417–422.

Dey, C. S., P. R. Deitiker, and H. F. Epstein. 1992. Assembly-dependent phosphorylation of myosin and paramyosin of native thick filaments in *Caenorhabditis elegans*. *Biochem. Biophys. Res. Commun.* 186:1528–1532.

Epstein, H. F., and D. A. Fischman. 1991. Molecular analysis of protein assembly in muscle development. *Science (Wash. DC).* 251:1039–1044.

Epstein, H. F., D. M. Miller, I. Ortiz, and G. C. Berliner. 1985. Myosin and paramyosin are organized around a newly identified core structure. *J. Cell Biol.* 100:904–915.

Epstein, H. F., I. Ortiz, and L. A. Traeger Mackinnon. 1986. The alteration of myosin isoform compartmentation in specific mutants of *Caenorhabditis elegans*. *J. Cell Biol.* 103:985–993.

Epstein, H. F., G. C. Berliner, and I. Ortiz. 1987. Assemblages of multiple thick filaments in nematodes. *J. Muscle Res. Cell Motil.* 8:527–536.

Epstein, H. F., G. C. Berliner, D. L. Casey, and I. Ortiz. 1988. Purified thick filaments from the nematode *Caenorhabditis elegans*: evidence for multiple proteins associated with core structures. *J. Cell Biol.* 106:1985–1995.

Epstein, H. F., D. L. Casey, and I. Ortiz. 1993. Myosin and paramyosin of *Caenorhabditis elegans* embryos assemble into nascent structures distinct from thick filaments and multi-filament assemblages. *J. Cell Biol.* 122:845–858.

Gengyo-Ando, K., and H. Kagawa. 1991. Single charge change on the helical surface of the paramyosin rod dramatically disrupts thick filament assembly in *Caenorhabditis elegans*. *J. Mol. Biol.* 219:429–441.

Harris, H. E., and H. F. Epstein. 1977. Myosin and paramyosin of *Caenorhabditis elegans*: biochemical and structural properties of wild type and mutant proteins. *Cell.* 15:709–719.

Honda, S., and H. F. Epstein. 1990. Modulation of muscle gene expression in *Caenorhabditis elegans*: differential levels of transcripts, mRNAs, and polypeptides for thick filament proteins during nematode development. *Proc. Natl. Acad. Sci. USA.* 87:876–880.

Huxley, H. E. 1963. Electron microscopy of native and synthetic protein filaments from striated muscle. *J. Mol. Biol.* 7:281–308.

Kagawa, H., K. Genkyo, A. D. McLachlan, S. Brenner, and J. Karn. 1989. Paramyosin gene (*unc-15*) of *Caenorhabditis elegans*. Molecular cloning, nucleotide sequence and models for thick filament structure. *J. Mol. Biol.* 207:311–333.

Levine, R. J. C., M. Elfvin, M. M. Dewey, and B. Walcott. 1976. Paramyosin in invertebrate muscles. II. Content in relation to structure and function. *J. Cell Biol.* 71:273–279.

Levine, R. J. C., R. W. Kensler, M. Stewart, and J. C. Haselgrove. 1982. Molecular organization of *Limulus* thick filaments. *In* Basic Biology of Muscles: A Comparative Approach. B. M. Twarog, R. J. C. Levine, and M. M. Dewey, editors. Raven Press, New York. pp. 37–52.

Levine, R. J. C., R. W. Kensler, M. C. Reedy, W. Hofmann, and H. A. King. 1983. Structure and paramyosin content of tarantula thick filaments. *J. Cell Biol.* 97:186–195.

Levine, R. J. C., R. W. Kensler, and P. Levitt. 1986. Crossbridge and backbone structure of invertebrate thick filaments. *Biophys. J.* 49:135–138.

Mackenzie, J. M., and H. F. Epstein. 1980. Paramyosin is necessary for determination of nematode thick filament length in vivo. *Cell.* 22:747–755.

McLachlan, A. D., and J. Karn. 1982. Periodic charge distribution in the myosin rod amino acid sequence match cross-bridge spacings in muscle. *Nature (Lond.).* 299:226–231.

McLachlan, A. D., and J. Karn. 1983. Periodic features in the amino acid sequence of the nematode myosin rod. *J. Mol. Biol.* 164:605–626.

Miller, D. M., I. Ortiz, G. C. Berliner, and H. F. Epstein. 1983. Differential localization of two myosins within nematode thick filaments. *Cell.* 34: 477–490.

Morimoto, K., and W. F. Harrington. 1973. Isolation and composition of rabbit skeletal thick filaments. *J. Mol. Biol.* 77:165–175.

Schachat, F., R. L. Garcea, and H. F. Epstein. 1978. Myosins exist as homodimers of heavy chains: demonstration with specific antibody purified by nematode mutant myosin affinity chromatography. *Cell.* 15:405–411.

Schriefer, L., and R. H. Waterston. 1989. Phosphorylation of the N-terminal region of *Caenorhabditis elegans* paramyosin. *J. Mol. Biol.* 207:451–454.

Szent-Györgyi, A., C. Cohen, and J. Kendrick-Jones. 1971. Paramyosin and the filaments of molluscan "catch" muscles. II. Native filaments: isolation and characterization. *J. Mol. Biol.* 56:239–258.

Vibert, P., and L. Castellani. 1989. Substructure and accessory proteins in scallop myosin filaments. *J. Cell Biol.* 109:539–547.

Waterston, R. H., H. F. Epstein, and S. Brenner. 1974. Paramyosin of *Caenorhabditis elegans*. *J. Mol. Biol.* 90:285–290.

Waterston, R. H., R. M. Fishpool, and S. Brenner. 1977. Mutants affecting paramyosin in *Caenorhabditis elegans*. *J. Mol. Biol.* 117:679–697.

Waterston, R. H. 1989. The minor myosin heavy chain, mhcA, of *Caenorhabditis elegans* is necessary for the initiation of thick filament assembly. *EMBO (Eur. Mol. Biol. Organ.) J.* 8:3429–3436.